

Interpreting the Weight Space of Customized Diffusion Models

Amil Dravid^{*1,2}Yossi Gandelsman^{*1}Kuan-Chieh Wang²Rameen Abdal³Gordon Wetzstein³Alexei A. Efros¹Kfir Aberman²¹UC Berkeley ²Snap Inc. ³Stanford University

Figure 1: *weights2weights (w2w) space enables generative applications on model weights*. We model a manifold of customized diffusion model weights as a subspace encoding different human identities. This forms a space that supports inverting the visual identity from a single image into a model, editing the identity encoded in the model, and sampling new models that encode diverse instances of people. This space effectively serves as a latent space over customized models.

Abstract

We investigate the space of weights spanned by a large collection of customized diffusion models. We populate this space by creating a dataset of over 60,000 models, each of which is a base model fine-tuned to insert a different person’s visual identity. We model the underlying manifold of these weights as a subspace, which we term *weights2weights*. We demonstrate three immediate applications of this space – sampling, editing, and inversion. First, as each point in the space corresponds to an identity, sampling a set of weights from it results in a model encoding a novel identity. Next, we find linear directions in this space corresponding to semantic edits of the identity (e.g., adding a beard). These edits persist in appearance across generated samples. Finally, we show that inverting a single image into this space reconstructs a realistic identity, even if the input image is out of distribution (e.g., a painting). Our results indicate that the weight space of fine-tuned diffusion models behaves as an interpretable latent space of identities.¹

^{*}Equal contribution; correspondence to amil_dravid@berkeley.edu

¹Project page: <https://snap-research.github.io/weights2weights/>

Code: <https://github.com/snap-research/weights2weights>

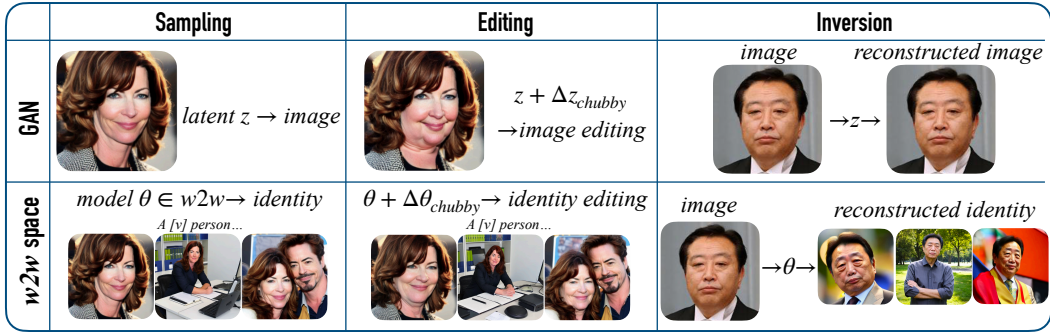


Figure 2: **The *weights2weights* space enables GAN-like applications on identity-encoding model weights.** Novel identities can be sampled from the space and edited by linearly traversing along semantic directions in weight space. Additionally, a single image can be inverted into the space to produce a model that consistently generates that identity.

1 Introduction

Generative models have emerged as a powerful tool to model our rich visual world. In particular, the latent space of single-step generative models, such as Generative Adversarial Networks (GANs) [15, 26], has been shown to linearly encode meaningful concepts in the output images. For instance, linear directions in GANs encode different attributes (e.g., gender or age of faces) and can be composed for multi-attribute image edits [17, 22, 56]. Alas, in multi-step generative models, like diffusion models [19, 57], such a linear latent space is yet to be found.

Recently introduced personalization approaches, such as Dreambooth [50] or Custom Diffusion [31], may hint at where such an interpretable latent space can exist in diffusion models. These methods aim to learn an instance of a subject, such as a person’s visual identity. Rather than searching for a latent code that represents an identity in the input noise space, these approaches customize diffusion models by fine-tuning on subject images, which results in identity-specific model weights. We therefore hypothesize that a latent space can exist *in the weights themselves*.

To test our hypothesis, we fine-tune over 60,000 personalized models on individual identities to obtain points that lie on a manifold of customized diffusion model weights. To reduce the dimensionality of each data point, we use low-rank approximation (LoRA) [20] during fine-tuning and further apply Principal Components Analysis (PCA) to the set of data points. This forms our final space: *weights2weights* ($w2w$). Unlike GANs, which model the pixel space of images, we model the *weight space* of these personalized models. Thus, each sample in our space corresponds to an identity-specific model which can consistently generate that subject. We provide a schematic in Fig. 2 that contrasts the GAN latent space with our proposed $w2w$ space, demonstrating the differences and analogies between these two representations.

Creating this space unlocks a variety of applications that involve traversal in $w2w$ (Fig. 1). First, we demonstrate that sampling model weights from $w2w$ space corresponds to a new identity. Second, we find linear directions in this space corresponding to semantic edits of the identity. Finally, we show that enforcing weights to live in this space enables a diffusion model to learn an identity given a single image, even if it is out of distribution.

We find that $w2w$ space is highly expressive through quantitative evaluation on editing customized models and encoding new identities given a single image. Qualitatively, we observe this space supports sampling models that encode diverse and realistic identities, while also capturing the key characteristics of out-of-distribution identities.

2 Related Work

Image-based generative models. Various models have been proposed for image generation, including Variational Autoencoders (VAEs) [29], Flow-based models [10, 30, 45], Generative Adversarial Networks (GANs) [15], and Diffusion models [19, 39, 57]. Within the realm of high-quality photo-realistic image generation, GANs [23, 26, 27] and Diffusion models [19, 39, 48, 58] have garnered

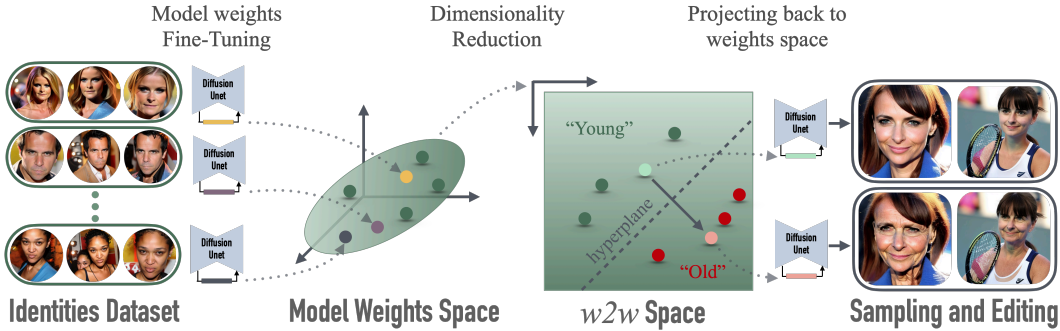


Figure 3: **Building weights2weights ($w2w$) space.** We create a dataset of model weights where each model is personalized to a specific identity using low-rank updates (LoRA). These model weights lie on a weights manifold that we further project into a lower-dimensional subspace spanned by its principal components. We train linear classifiers to find disentangled edit directions in this space.

significant attention due to their controllability and ability to produce high-quality images. Leveraging the compositionality of these models, methods for personalization and customization have been developed which aim to insert user-defined concepts via fine-tuning [13, 31, 36, 50]. Various works try to reduce the dimensionality of the optimized parameters for personalization either by operating in specific model layers [31] or in text-embedding space [13], by training hypernetworks [51], and by constructing a linear basis in text embedding space [66].

Latent space of generative models. Linear latent space models of facial shape and appearance were studied extensively in the 1990s, using both PCA-based representations (e.g. Active Appearance Models [7], 3D Morphable Models [4]) as well as models operating directly in pixel and keypoint space [49]. However, these techniques were restricted to aligned and cropped frontal faces. More recently, Generative Adversarial Networks (GANs), particularly the StyleGAN series [24, 25, 26, 27], have showcased editing capabilities facilitated by their interpretable latent space. Furthermore, linear directions can be found in their latent space to conduct semantic edits by training linear classifiers or applying PCA [17, 56], among other methods for discovering semantic directions [6, 60]. Several methods aim to project real images into the GAN latent space in order to conduct this editing [1, 47, 59, 69].

Although diffusion models architecturally lack such a latent space, some works aim to discover a GAN-like latent space in them. This has been explored in the UNet bottleneck layer [32, 37], noise space [8], and text-embedding space [3]. Concept Sliders [14] explores the weight space for semantic image editing by conducting low-rank training with contrasting image or text pairs.

Weights as data. Past works have exploited the structure within weight space of deep networks for various applications. In particular, some have found linear properties of weights, enabling simple model ensembling and editing via arithmetic operations [21, 52, 55, 63]. Other works create datasets of neural network parameters for training hypernetworks [11, 16, 38, 51, 62], predicting properties of networks [54], and creating design spaces for models [42, 43].

3 Method

We start by demonstrating how we create a manifold of model weights as illustrated in Fig. 3. We explain how we obtain low-dimensional data points for this space, each of which represents an individual identity. We then use these points to model a weights manifold. Next, we find linear directions in this manifold that correspond to semantic attributes and use them for editing the identities. Finally, we demonstrate how this manifold can be utilized for constraining an ill-posed inversion task with a single image to reconstruct its identity.

3.1 Preliminaries

In this section, we first introduce latent diffusion models (LDM) [48], which we will use to create a dataset of weights. Then, we explain the approach for obtaining identity-specific models from LDM via Dreambooth [50] fine-tuning. We finally present a version of fine-tuning that uses low-dimensional weight updates (LoRA [20]). We will use the fine-tuned low-dimensional per-identity weights as data points to construct the weights manifold in Sec. 3.2.

Latent diffusion models [48]. We will extract weights from latent diffusion models to create $w2w$ space. These models follow the standard diffusion objective [19] while operating on latents extracted from a pre-trained Variational Autoencoder [12, 29, 46]. With text, the conditioning signal is encoded by a text encoder (such as CLIP [40]), and the resulting embeddings are provided to the denoising UNet model. The loss of latent diffusion models is:

$$\mathbb{E}_{\mathbf{x}, \mathbf{c}, \epsilon, t} [w_t \|\epsilon - \epsilon_\theta(\mathbf{x}_t, \mathbf{c}, t)\|_2^2], \quad (1)$$

where ϵ_θ is the denoising UNet, \mathbf{x}_t is the noised version of the latent for an image, \mathbf{c} is the conditioning signal, t is the diffusion timestep, and w_t is a time-dependent weight on the loss.

To sample from the model, a random Gaussian latent x_T is deterministically denoised conditioned on a prompt for a fixed set of timesteps with a DDIM sampler [58]. The denoised latent is then fed through the VAE decoder to generate the final image.

Dreambooth [50]. To obtain an identity-specific model, we use the Dreambooth personalization method. Dreambooth fine-tuning introduces a novel subject into a pre-trained diffusion model given only a few images of it. During training, Dreambooth follows a two-part objective:

$$\mathbb{E}_{\mathbf{x}, \mathbf{c}, \epsilon, t} [w_t \|\epsilon - \epsilon_\theta(\mathbf{x}_t, \mathbf{c}, t)\|_2^2 + \lambda w_{t'} \|\epsilon' - \epsilon_\theta(\mathbf{x}'_t, \mathbf{c}', t')\|_2^2], \quad (2)$$

where the first term corresponds to the standard diffusion denoising objective using the subject-specific data \mathbf{x} conditioned on the text prompt “[identifier] [class noun]” (e.g., “[v] person”), denoted \mathbf{c} . The second term, weighted by λ , corresponds to a prior preservation loss, which involves the standard denoising objective using the model’s own generated samples \mathbf{x}' for the broader class \mathbf{c}' (e.g., “person”). This prevents the model from associating the class name with the specific instance, while also leveraging the semantic prior on the class. We utilize this approach to obtain a per-subject model and use its weights to create the interpretable weights manifold.

Low Rank Adaptation (LoRA) [20]. Dreambooth requires fine-tuning all the weights of a model, which is a high-dimensional space. We turn to a more efficient fine-tuning scheme, LoRA, that modifies only a low-rank version of the weights. LoRA uses weight updates ΔW with a low intrinsic rank. For a base model layer $W \in \mathbb{R}^{m \times n}$, the LoRA update for that layer ΔW can be decomposed into $\Delta W = BA$, where $B \in \mathbb{R}^{m \times r}$ and $A \in \mathbb{R}^{r \times n}$ are low-rank matrices with $r \ll \min(m, n)$. During training, for each model layer, only the A and B are updated. This significantly reduces the number of trainable parameters. During inference, the low-rank weights are added residually to the weights of each layer in the base model and scaled by a coefficient $\alpha \in \mathbb{R}$: $W + \alpha \Delta W$.

3.2 Constructing the weights manifold

Creating a dataset of model weights. To construct the *weights2weights* ($w2w$) space, we begin by creating a dataset of model weights θ_i . We conduct Dreambooth fine-tuning on Latent Diffusion models in order to insert new subjects with the ability to control image instances using text prompts. This training is done with LoRA in order to reduce the space of model parameters. Each model is fine-tuned on a set of images corresponding to one human subject. After training, we flatten and concatenate all of the LoRA matrices, resulting in a data point $\theta_i \in \mathbb{R}^d$ which represents one identity. After training over N different instances, we have our final dataset of model weights $\mathcal{D} = \{\theta_1, \theta_2, \dots, \theta_N\}$, representing a diverse array of subjects.

Modeling the weights manifold. We posit that our data $\mathcal{D} \subseteq \mathbb{R}^d$ lies on a lower-dimensional manifold of weights that encode identities. A randomly sampled set of weights in \mathbb{R}^d , would not be guaranteed to produce a valid model encoding identity as the d degrees of freedom can be fine-tuned for any purpose. Therefore, we hypothesize that this manifold is a subset of the weight space. Inspired by findings that high-level concepts can be encoded as linear subspaces of representations [34, 41, 44], we model this subset as a linear subspace \mathbb{R}^m where $m < d$, and call it *weights2weights* ($w2w$) space. We represent points in this subspace as a linear combination of basis vectors $\mathbf{w} = \{w_1, \dots, w_m\}$, $w_i \in \mathbb{R}^d$. In practice, we apply Principal Component Analysis (PCA) on the N models and keep the first m principal components for dimensional reduction and forming our basis of m vectors.

Sampling from the weights manifold. After modeling this weights manifold, we can sample a new model that lies on it, resulting in a new model that generates a novel identity. We sample a model represented with basis coefficients $\{\beta_1, \dots, \beta_m\}$, where each coefficient β_k is sampled from a normal distribution with mean μ_k and standard deviation σ_k . The mean and standard deviation are calculated for each principal component k from the coefficients among all the training models.

3.3 Finding Interpretable Weight Space Directions

We seek a direction $\mathbf{n} \in \mathbb{R}^d$ defining a hyperplane that separates between binary identity properties embedded in the model weights (e.g., male/female), similarly to hyperplanes observed in the latent space of GANs [56]. We assume binary labels are given for attributes present in the identities encoded by the models. We then train linear classifiers using weights of the models as data based on these labels, imposing separating hyperplanes in weight space. Given an identity parameterized by weights θ , we can manipulate a single attribute by traversing in a direction \mathbf{n} , orthogonal to the separating hyperplane: $\theta_{\text{edit}} = \theta + \alpha \mathbf{n}$.

3.4 Inversion into $w2w$ Space

Traditionally, inversion of a generative model involves finding an input such as a latent code that best reconstructs a given image [35, 64]. This corresponds to finding a projection of the input onto the learned data manifold [69]. With $w2w$ space, we model a manifold of data which happens to be model weights rather than images. Inspired by latent optimization methods [1, 69], we propose a gradient-based method of inverting a single identity from an image into our discovered space.

Given a single image \mathbf{x} , we follow a constrained denoising objective:

$$\max_{\theta} \mathbb{E}_{\mathbf{x}, \mathbf{c}, \epsilon, t} [w_t \| \epsilon - \epsilon_{\theta}(\mathbf{x}_t, \mathbf{c}, t) \|_2^2] \quad \text{s.t. } \theta \in w2w \quad (3)$$

Specifically, we constrain the model weights to lie in $w2w$ space by optimizing a set of basis coefficients $\{\beta_1, \dots, \beta_m\}$ rather than the original parameters. Unlike Dreambooth, we do not employ a prior preservation loss, since the optimized model lies in the subspace defined by our dataset of weights, and inherits their priors.

4 Experiments

We demonstrate $w2w$ space on human identities for a variety of applications. We begin by detailing implementation details. Next, we use $w2w$ space for 1) sampling new models encoding novel identities, 2) editing identity attributes in a consistent manner via linear traversal in $w2w$ space, 3) embedding a new identity given a single image, and 4) projecting out-of-distribution identities into $w2w$ space. Finally, we analyze how scaling the number of models in our dataset of model weights affects the disentanglement of attribute directions and preservation of identity. We refer the reader to Appendix H, where we apply $w2w$ space to other visual concepts.

4.1 Implementation Details

Creating an identity dataset. We generate a synthetic dataset of $\sim 65,000$ identities using [61], where each identity is associated with multiple images of that person. Each identity is based on an image with labeled binary attributes (e.g., male/female) from CelebA [33]. Each set of images corresponding to an identity is then used as data to fine-tune a latent diffusion model with Dreambooth. Note that the same identity can occur multiple times in different images in CelebA. As such, some of our generated identities may encode different instances of the same person. This results in some of the fine-tuned models in our dataset of weights encoding different instances of the same person. Further details are provided in Appendix E.

Encoding identities into model weights. We conduct Dreambooth fine-tuning using LoRA with rank 1 on the identities. Following [31, 52], we only fine-tune the key and value projection matrices in the cross-attention layers. We utilize the RealisticVision-v51² checkpoint based on Stable Diffusion 1.5. Conducting Dreambooth fine-tuning on each identity training set results in a dataset of $\sim 65,000$ weights θ where $\theta \in \mathbb{R}^{100,000}$. We hold out 100 identities for evaluating edits, which results in leaving out ~ 1000 models based on how we constructed our identity datasets.

Finding semantic attribute directions. We utilize binary attribute labels from CelebA to train linear classifiers on the dataset of model weights we curated. We run Principal Component Analysis (PCA) on the $\sim 65,000$ training models and project to the first 1000 principal components in order to

²<https://huggingface.co/stablediffusionapi/realistic-vision-v51>

reduce the dimensionality. The orthogonal edit directions are calculated via the analytic least squares solution on the matrix of projected training models $\mathcal{D} \in \mathbb{R}^{65,000 \times 1000}$, and then unprojected to the original dimensionality of the model weights: $\theta \in \mathbb{R}^{100,000}$.

4.2 Sampling from $w2w$ Space

We present images generated from models that were sampled from the weights manifold (i.e., $w2w$ Space) in Fig. 4. We follow the sampling procedure from Sec. 3.2, and generate images from the sampled model with various prompts and seeds. As shown, each new model encodes a novel, realistic, and consistent identity. Additionally, we present the nearest neighbor model among the training dataset of model weights. We use cosine similarity on the models’ principal component representations. Comparing with the nearest neighbors shows that these samples are not just copies from the dataset, but rather encode diverse identities with different attributes. Yet, the samples still demonstrate some similar features to the nearest neighbors. These include jawline and eye shape (top row), facial hair (middle row), and nose and eye shape (bottom row). Appendix A includes more such examples.

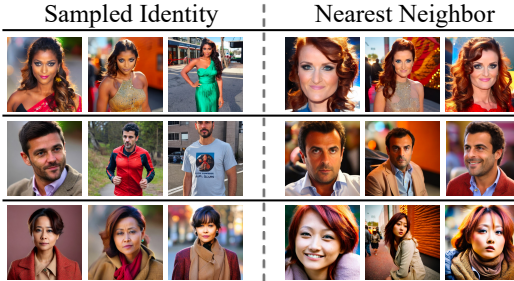


Figure 4: **Identity samples from $w2w$ space.** We show the samples from $w2w$ space do not overfit to nearest-neighbor identities, although they incorporate facial attributes from them. The identities are diverse and consistent across generations.

4.3 Editing Subjects

We demonstrate how directions found by the linear classifiers can be used to edit subjects encoded in the models. It is desired that these edits are 1) disentangled (i.e., do not interfere with other attributes of the embedded subject and preserve all other concepts such as context) 2) identity preserving (i.e., the person is still recognizable) 3) and semantically aligned with the intended edit.

Baselines. We compare against a naïve baseline of prompting with the desired attribute (e.g., “[v] person with small eyes”), and then Concept Sliders [14], an instance-specific editing method which we adapt to subject editing. In particular, we train their most accessible method, the text-based slider, which trains LoRAs to modulate attributes in a pretrained diffusion model based on contrasting text prompts. We then apply these sliders to the personalized identity models.

Evaluation protocol. We evaluate these three methods for identity preservation, disentanglement, and edit coherence. To measure identity preservation, we first detect faces in the original generated images and the result of the edits using MTCNN [67]. We then calculate the similarity of the FaceNet [53] embeddings. We also use LPIPS [68] computed between the images before and after



Figure 5: **Qualitative comparison.** $w2w$ edits preserve identity while being disentangled and semantically aligned. Concept Sliders [14] tends to exaggerate effects which induces artifacts and degrades identity, while prompting the subject with the desired edit has unexpected effects.

Table 1: Edits in $w2w$ space preserve identity, are disentangled, and semantically aligned.

	ID Score \uparrow			Prompting	LPIPS \downarrow			CLIP Score \uparrow		
	Prompting	Sliders	$w2w$		Sliders	$w2w$	Prompting	Sliders	$w2w$	
Gender	0.39 \pm 0.08	0.33 \pm 0.09	0.45 \pm 0.09	0.30 \pm 0.05	0.39 \pm 0.09	0.31 \pm 0.03	1.98 \pm 0.78	3.50 \pm 0.68	4.13 \pm 0.59	
Chubby	0.29 \pm 0.14	0.33 \pm 0.09	0.45 \pm 0.09	0.41 \pm 0.05	0.38 \pm 0.04	0.36 \pm 0.04	1.12 \pm 0.61	2.21 \pm 0.61	2.16 \pm 0.51	
Eyes	0.52 \pm 0.06	0.53 \pm 0.04	0.72 \pm 0.05	0.32 \pm 0.03	0.30 \pm 0.02	0.19 \pm 0.02	0.17 \pm 0.17	0.01 \pm 0.22	0.59 \pm 0.19	



Figure 6: **Composing multiple attributes persist in appearance.** We demonstrate how we can apply multiple edits in $w2w$ space without significant degradation of the original identity or interference with other concepts. These edits persist and maintain their appearance across different generation seeds and prompts.

the edit to measure the degree of disentanglement with other visual elements, and CLIP score [18], to measure if the desired edit matches the text caption for the edit.

To generate samples, we fix a set of prompts and random seeds which are used as input to the held-out identity models. Then, we choose a set of identity-specific manipulations. For prompt-based editing, we augment the attribute description to the set of fixed prompts (e.g., “chubby [v] person”). For Concept Sliders and $w2w$, we apply the weight space edit directions to the personalized model with a fixed norm which determines the edit strength. The norm is calculated using the maximum projection component onto the edit direction among the training set of model weights.

$w2w$ edits are identity preserving and disentangled. We evaluate over a range of identity-specific attributes and present three (gender, chubby, narrow eyes) in Tab. 1. Edits in $w2w$ preserve the identity of the original subject as measured by the ID score. These edits are semantically aligned with the desired effect as indicated by the CLIP score while minimally interfering with other visual concepts, as measured by LPIPS. We note that the CLIP score can be noisy in this setting as text captions can be too coarse to describe attributes as nuanced as those related to the human face.

Qualitatively, $w2w$ edits make the minimal amount of changes to achieve semantic and identity-preserving edits (Fig. 5). For instance, changing the gender of the man does not significantly change the facial structure or hair, unlike Concept Sliders or prompting with text descriptions. Prompting has inconsistent results, either creating no effect or making drastic changes. Concept Sliders tends to make caricaturized effects, such as making the man cartoonishly chubby and baby-like.

Composing edits. Edit directions in $w2w$ space can be composed linearly as shown in Fig. 6. The composed edits persist in appearance across different generations, binding to the identity. Furthermore, the edited weights result in a new model, where the subject has different attributes while still maintaining as much of the prior identity. As we operate on a weight manifold, minimal changes are made to other concepts, such as scene layout or other people. For instance, in Fig. 6, adding edits to the woman does not interfere with Obama standing by her.

4.4 Inverting Subjects

Evaluation protocol. We measure $w2w$ space’s ability to represent novel identities by inverting a set of 100 random FFHQ [26] face images. We follow our inversion objective from eq. 3. We then provide a set of diverse prompts to generate multiple images and follow the identity preservation metric from Sec. 4.3 to measure subject fidelity. Implementation details are provided in Appendix C.

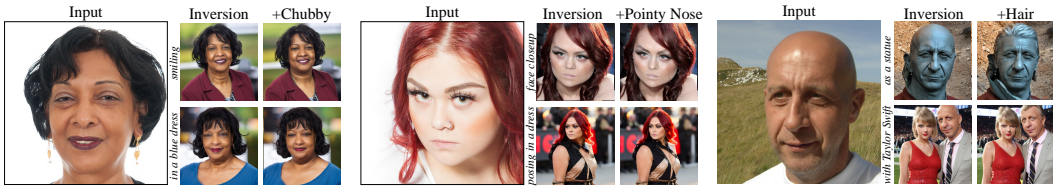


Figure 7: **Single image inversion reconstructs identity and enables editing in $w2w$ space.** Inverted identities can be composed in novel contexts. Additionally, applying our discovered semantic directions edits attributes that persist in appearance across generation seeds and prompts.

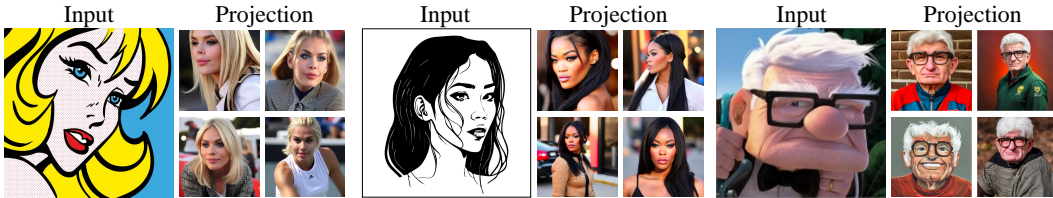


Figure 8: **Projecting out-of-distribution identities.** We show that our inversion method can convert unrealistic identities into realistic renderings with in-domain facial features. The resulting identity can be composed in novel scenes, such as playing tennis or rendered into other artistic domains.

We compare our results to two approaches that use Dreambooth with rank-1 LoRA. The first is trained on a single image. The second is trained on *multiple images of each identity*. We generate such images by following our identity dataset construction from Sec. 4.1). This approach can be viewed as a pseudo-upper bound on modeling identity as it uses multiple images.

$w2w$ space provides a strong identity prior. Inverting a single image into $w2w$ space improves on the single image Dreambooth baseline and closes the gap with the Dreambooth baseline that uses multiple identity images (Tab. 2). Conducting Dreambooth fine-tuning with a single image in the original weight space leads to image overfitting and poor subject reconstruction as indicated by a lower ID score. In contrast, by constraining the optimized weights to lie on a manifold of identity weights, $w2w$ inversion inherits the rich priors of the models used to discover the space. As such, it can extract a high-fidelity identity that is consistent and compositional across generations. We present qualitative comparisons against Dreambooth and single-image Dreambooth in Appendix C.

Inverted models are editable. Fig. 7 demonstrates that a diverse set of identities can be faithfully represented in $w2w$ space. After inversion, the encoded identity can be composed in novel contexts and poses. For instance, the inverted man (rightmost example) can be seen posing with Taylor Swift or rendered as a statue. Moreover, semantic edits can be applied to the inverted models while maintaining appearance across generations.

Table 2: **$w2w$ Inversion closes the gap with Dreambooth.**

Method	Single-Image	ID Score \uparrow
DB-LoRA	×	0.69 \pm 0.01
DB-LoRA	✓	0.43 \pm 0.03
$w2w$	✓	0.64 \pm 0.01

4.5 Out-of-Distribution Projection

$w2w$ space captures out-of-distribution identities. We follow the $w2w$ inversion method from Sec. 4.4 to project images of unrealistic identities (e.g., paintings, cartoons, etc.) onto the weights manifold, and present these qualitative results in Fig. 8. By constraining the optimized model to live in $w2w$ space, the inverted identities are converted into realistic renditions of the stylized identities, capturing prominent facial features. In Fig. 8, notice how the inverted identities generate a similar blonde hairstyle and nose structure in the first example, defined jawline and lip shape in the second example, and head shape and big nose in the last example. As also shown in the figure, the inverted identities can also be translated to other artistic domains using text prompts. We present a variety of domains projected into $w2w$ space in Appendix D.

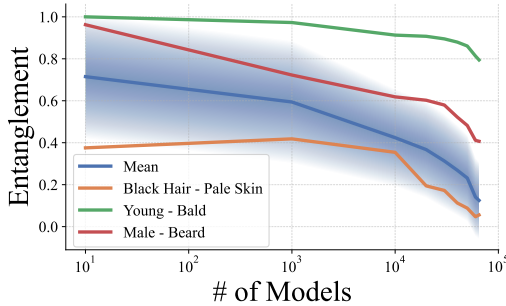


Figure 9: **Scaling our model weights further disentangles classifier directions.** We highlight the trend in disentanglement of three examples where attributes may be strongly correlated among identities. As the number of models (*Identities*) is increased, the features are less entangled.

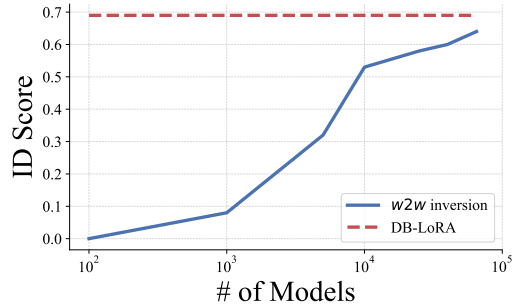


Figure 10: **Scaling the number of models improves identity preservation.** As the span of $w2w$ space increases, inversion can reconstruct single-image identities more faithfully, approaching the pseudo-upper bound of multi-image Dreambooth (DB-LoRA).

4.6 Effect of Number of Models Spanning $w2w$ Space

We ablate the number of models used to create $w2w$ space and investigate the expressiveness of the resulting space. In particular, we measure the degree of entanglement among the edit direction and how well this space can capture identity.

Disentanglement vs. the number of models. We find that scaling the number of models in our dataset of weights leads to less entangled edit directions in $w2w$ space (Fig. 9). We vary the number of models in our dataset of weights and reapply PCA to establish a basis. We then measure the absolute value of cosine similarity (lower is better) between all pairs of linear classifier directions found for CelebA labels. We repeat this as we scale the number of model weights used to train the classifiers. We report the mean and standard deviation for these scores, along with three notable semantic direction pairs. We observe a trend in decreasing cosine similarity. Notably, pairs such as “Black Hair - Pale Skin,” “Young - Bald,” and “Male - Beard” which may correlate in the distribution of identities, become less correlated as we scale our dataset of model weights.

Identity preservation vs. the number of models. We observe that as we scale the number of models in our dataset of weights, identities are more faithfully represented in $w2w$ space (Fig. 10). We follow the same procedure as the disentanglement ablation, reapplying PCA to establish a basis based on the dataset of model weights. Next, following Sec. 4.4, we optimize coefficients for this basis and measure the average ID score over the 100 inverted FFHQ evaluation identities. As each model in our dataset encodes a different instance of an identity, growing this dataset increases the span of $w2w$ space and its ability to capture more diverse identities. We plot the average multi-image Dreambooth LoRA (DB-LoRA) ID score from Sec. 4.4, which is agnostic to our dataset of models. This establishes a pseudo-upper bound on identity preservation. Scaling enables $w2w$ to represent identities given a single image with performance approaching that of traditional Dreambooth with LoRA, which uses multiple images and trains in a higher dimensional space.

5 Limitations

As with any data-driven method, $w2w$ space inherits the biases of the data used to discover it. For instance, co-occurring attributes in the identity-encoding models would cause linear classifier directions to entangle them (e.g. gender and facial hair). However, as we scale the number of models, spurious correlations will drop as evidenced by Fig. 9. These directions are also limited by the labels present in CelebA. Additionally, the span of the $w2w$ space is dictated by the models used to create it. Thus, $w2w$



Figure 11: *weights2weights* fails to capture identities with undersampled attributes.

space can struggle to represent more complex identities as seen in Fig. 11. Inversion in these cases amounts to projecting onto the closest identity on the weights manifold. Despite these limitations, our analysis on the size of the model dataset reveals that forming a space using a larger and more diverse set of identity-encoding models can mitigate this limitation.

6 Discussion and Broader Impact

We presented a paradigm for representing diffusion model weights as a point in a space defined by other customized models – *weights2weights* ($w2w$) space. This enabled applications analogous to those of a generative latent space – inversion, editing, and sampling – but producing model weights rather than images. We demonstrated these applications on model weights encoding human identities. Although these applications could enable malicious manipulation of real human identities, we hope the community uses the framework to explore visual creativity as well as utilize this interpretable space for controlling models for safety. We hypothesize that such a framework can generalize to other concepts, beyond faces and identities (see Appendix H). We plan to further investigate the generality of *weights2weights* in future work.

Acknowledgements

The authors would like to thank Grace Luo, Lisa Dunlap, Konpat Preechakul, Sheng-Yu Wang, Stephanie Fu, Or Patashnik, Daniel Cohen-Or, and Sergey Tulyakov for helpful discussions. AD is supported by the US Department of Energy Computational Science Graduate Fellowship. Part of the work was completed by AD as an intern with Snap Inc. YG is funded by the Google Fellowship. Additional funding came from ONR MURI.

References

- [1] Rameen Abdal, Yipeng Qin, and Peter Wonka. Image2stylegan: How to embed images into the stylegan latent space? In *Proceedings of the IEEE/CVF international conference on computer vision*, pages 4432–4441, 2019.
- [2] Josh Achiam, Steven Adler, Sandhini Agarwal, Lama Ahmad, Ilge Akkaya, Florencia Leoni Aleman, Diogo Almeida, Janko Altenschmidt, Sam Altman, Shyamal Anadkat, et al. Gpt-4 technical report. *arXiv preprint arXiv:2303.08774*, 2023.
- [3] Stefan Andreas Baumann, Felix Krause, Michael Neumayr, Nick Stracke, Vincent Tao Hu, and Björn Ommer. Continuous, subject-specific attribute control in t2i models by identifying semantic directions. *arXiv preprint arXiv:2403.17064*, 2024.
- [4] Volker Blanz and Thomas Vetter. A morphable model for the synthesis of 3d faces. In *Proceedings of the 26th Annual Conference on Computer Graphics and Interactive Techniques, SIGGRAPH '99*, page 187–194, USA, 1999. ACM Press/Addison-Wesley Publishing Co.
- [5] Mingdeng Cao, Xintao Wang, Zhongang Qi, Ying Shan, Xiaohu Qie, and Yinqiang Zheng. Masactrl: Tuning-free mutual self-attention control for consistent image synthesis and editing. In *Proceedings of the IEEE/CVF International Conference on Computer Vision*, pages 22560–22570, 2023.
- [6] Anton Cherepkov, Andrey Voynov, and Artem Babenko. Navigating the gan parameter space for semantic image editing. In *Proceedings of the IEEE/CVF conference on computer vision and pattern recognition*, pages 3671–3680, 2021.
- [7] Timothy F Cootes, Gareth J Edwards, and Christopher J Taylor. Active appearance models. In *Computer Vision—ECCV'98: 5th European Conference on Computer Vision Freiburg, Germany, June 2–6, 1998 Proceedings, Volume II 5*, pages 484–498. Springer, 1998.
- [8] Yusuf Dalva and Pinar Yanardag. Noiseclr: A contrastive learning approach for unsupervised discovery of interpretable directions in diffusion models. *arXiv preprint arXiv:2312.05390*, 2023.

- [9] Jia Deng, Wei Dong, Richard Socher, Li-Jia Li, Kai Li, and Li Fei-Fei. Imagenet: A large-scale hierarchical image database. In *2009 IEEE conference on computer vision and pattern recognition*, pages 248–255. Ieee, 2009.
- [10] Laurent Dinh, Jascha Sohl-Dickstein, and Samy Bengio. Density estimation using real nvp. In *International Conference on Learning Representations*, 2016.
- [11] Ziya Erkoç, Fangchang Ma, Qi Shan, Matthias Nießner, and Angela Dai. Hyperdiffusion: Generating implicit neural fields with weight-space diffusion. In *Proceedings of the IEEE/CVF International Conference on Computer Vision*, pages 14300–14310, 2023.
- [12] Patrick Esser, Robin Rombach, and Bjorn Ommer. Taming transformers for high-resolution image synthesis. In *Proceedings of the IEEE/CVF conference on computer vision and pattern recognition*, pages 12873–12883, 2021.
- [13] Rinon Gal, Yuval Alaluf, Yuval Atzmon, Or Patashnik, Amit Haim Bermano, Gal Chechik, and Daniel Cohen-or. An image is worth one word: Personalizing text-to-image generation using textual inversion. In *The Eleventh International Conference on Learning Representations*, 2022.
- [14] Rohit Gandikota, Joanna Materzynska, Tingrui Zhou, Antonio Torralba, and David Bau. Concept sliders: Lora adaptors for precise control in diffusion models. *arXiv preprint arXiv:2311.12092*, 2023.
- [15] Ian Goodfellow, Jean Pouget-Abadie, Mehdi Mirza, Bing Xu, David Warde-Farley, Sherjil Ozair, Aaron Courville, and Yoshua Bengio. Generative adversarial nets. *Advances in neural information processing systems*, 27, 2014.
- [16] David Ha, Andrew M Dai, and Quoc V Le. Hypernetworks. In *International Conference on Learning Representations*, 2016.
- [17] Erik Härkönen, Aaron Hertzmann, Jaakko Lehtinen, and Sylvain Paris. Ganspace: Discovering interpretable gan controls. *arXiv preprint arXiv:2004.02546*, 2020.
- [18] Jack Hessel, Ari Holtzman, Maxwell Forbes, Ronan Le Bras, and Yejin Choi. Clipscore: A reference-free evaluation metric for image captioning. *arXiv preprint arXiv:2104.08718*, 2021.
- [19] Jonathan Ho, Ajay Jain, and Pieter Abbeel. Denoising diffusion probabilistic models. *Advances in neural information processing systems*, 33:6840–6851, 2020.
- [20] Edward J Hu, Phillip Wallis, Zeyuan Allen-Zhu, Yuanzhi Li, Shean Wang, Lu Wang, Weizhu Chen, et al. Lora: Low-rank adaptation of large language models. In *International Conference on Learning Representations*, 2021.
- [21] Gabriel Ilharco, Marco Tulio Ribeiro, Mitchell Wortsman, Ludwig Schmidt, Hannaneh Hajishirzi, and Ali Farhadi. Editing models with task arithmetic. In *The Eleventh International Conference on Learning Representations*, 2022.
- [22] Ali Jahanian, Lucy Chai, and Phillip Isola. On the "steerability" of generative adversarial networks. In *International Conference on Learning Representations*, 2019.
- [23] Minguk Kang, Jun-Yan Zhu, Richard Zhang, Jaesik Park, Eli Shechtman, Sylvain Paris, and Taesung Park. Scaling up gans for text-to-image synthesis. In *Proceedings of the IEEE/CVF Conference on Computer Vision and Pattern Recognition*, pages 10124–10134, 2023.
- [24] Tero Karras, Miika Aittala, Janne Hellsten, Samuli Laine, Jaakko Lehtinen, and Timo Aila. Training generative adversarial networks with limited data. *Advances in neural information processing systems*, 33:12104–12114, 2020.
- [25] Tero Karras, Miika Aittala, Samuli Laine, Erik Härkönen, Janne Hellsten, Jaakko Lehtinen, and Timo Aila. Alias-free generative adversarial networks. *Advances in neural information processing systems*, 34:852–863, 2021.
- [26] Tero Karras, Samuli Laine, and Timo Aila. A style-based generator architecture for generative adversarial networks. In *Proceedings of the IEEE/CVF conference on computer vision and pattern recognition*, pages 4401–4410, 2019.

- [27] Tero Karras, Samuli Laine, Miika Aittala, Janne Hellsten, Jaakko Lehtinen, and Timo Aila. Analyzing and improving the image quality of stylegan. In *Proceedings of the IEEE/CVF Conference on Computer Vision and Pattern Recognition*, pages 8110–8119, 2020.
- [28] Diederik P Kingma and Jimmy Ba. Adam: a method for stochastic optimization. In *International Conference on Learning Representations*, 2014.
- [29] Diederik P Kingma and Max Welling. Auto-encoding variational bayes. *International Conference on Learning Representations*, 2014.
- [30] Durk P Kingma and Prafulla Dhariwal. Glow: Generative flow with invertible 1x1 convolutions. *Advances in neural information processing systems*, 31, 2018.
- [31] Nupur Kumari, Bingliang Zhang, Richard Zhang, Eli Shechtman, and Jun-Yan Zhu. Multi-concept customization of text-to-image diffusion. In *Proceedings of the IEEE/CVF Conference on Computer Vision and Pattern Recognition*, pages 1931–1941, 2023.
- [32] Mingi Kwon, Jaeseok Jeong, and Youngjung Uh. Diffusion models already have a semantic latent space. In *The Eleventh International Conference on Learning Representations*, 2022.
- [33] Ziwei Liu, Ping Luo, Xiaogang Wang, and Xiaoou Tang. Deep learning face attributes in the wild. In *Proceedings of the IEEE international conference on computer vision*, pages 3730–3738, 2015.
- [34] Tomas Mikolov, Ilya Sutskever, Kai Chen, Greg S Corrado, and Jeff Dean. Distributed representations of words and phrases and their compositionality. *Advances in neural information processing systems*, 26, 2013.
- [35] Ron Mokady, Amir Hertz, Kfir Aberman, Yael Pritch, and Daniel Cohen-Or. Null-text inversion for editing real images using guided diffusion models. In *Proceedings of the IEEE/CVF Conference on Computer Vision and Pattern Recognition*, pages 6038–6047, 2023.
- [36] Yotam Nitzan, Kfir Aberman, Qiurui He, Orly Liba, Michal Yarom, Yossi Gandelsman, Inbar Mosseri, Yael Pritch, and Daniel Cohen-Or. Mystyle: A personalized generative prior. *ACM Transactions on Graphics (TOG)*, 41(6):1–10, 2022.
- [37] Yong-Hyun Park, Mingi Kwon, Jaewoong Choi, Junghyo Jo, and Youngjung Uh. Understanding the latent space of diffusion models through the lens of riemannian geometry. *Advances in Neural Information Processing Systems*, 36:24129–24142, 2023.
- [38] William Peebles, Ilija Radosavovic, Tim Brooks, Alexei A Efros, and Jitendra Malik. Learning to learn with generative models of neural network checkpoints. *arXiv preprint arXiv:2209.12892*, 2022.
- [39] Ryan Po, Wang Yifan, Vladislav Golyanik, Kfir Aberman, Jonathan T Barron, Amit H Bermano, Eric Ryan Chan, Tali Dekel, Aleksander Holynski, Angjoo Kanazawa, et al. State of the art on diffusion models for visual computing. *arXiv preprint arXiv:2310.07204*, 2023.
- [40] Alec Radford, Jong Wook Kim, Chris Hallacy, Aditya Ramesh, Gabriel Goh, Sandhini Agarwal, Girish Sastry, Amanda Askell, Pamela Mishkin, Jack Clark, et al. Learning transferable visual models from natural language supervision. In *International conference on machine learning*, pages 8748–8763. PMLR, 2021.
- [41] Alec Radford, Luke Metz, and Soumith Chintala. Unsupervised representation learning with deep convolutional generative adversarial networks. *arXiv preprint arXiv:1511.06434*, 2015.
- [42] Ilija Radosavovic, Justin Johnson, Saining Xie, Wan-Yen Lo, and Piotr Dollár. On network design spaces for visual recognition. In *Proceedings of the IEEE/CVF international conference on computer vision*, pages 1882–1890, 2019.
- [43] Ilija Radosavovic, Raj Prateek Kosaraju, Ross Girshick, Kaiming He, and Piotr Dollár. Designing network design spaces. In *Proceedings of the IEEE/CVF conference on computer vision and pattern recognition*, pages 10428–10436, 2020.

- [44] Shauli Ravfogel, Yanai Elazar, Hila Gonen, Michael Twiton, and Yoav Goldberg. Null it out: Guarding protected attributes by iterative nullspace projection. In *Proceedings of the 58th Annual Meeting of the Association for Computational Linguistics*, pages 7237–7256, 2020.
- [45] Danilo Rezende and Shakir Mohamed. Variational inference with normalizing flows. In *International conference on machine learning*, pages 1530–1538. PMLR, 2015.
- [46] Danilo Jimenez Rezende, Shakir Mohamed, and Daan Wierstra. Stochastic backpropagation and approximate inference in deep generative models. In *International conference on machine learning*, pages 1278–1286. PMLR, 2014.
- [47] Daniel Roich, Ron Mokady, Amit H Bermano, and Daniel Cohen-Or. Pivotal tuning for latent-based editing of real images. *ACM Transactions on graphics (TOG)*, 42(1):1–13, 2022.
- [48] Robin Rombach, Andreas Blattmann, Dominik Lorenz, Patrick Esser, and Björn Ommer. High-resolution image synthesis with latent diffusion models. In *Proceedings of the IEEE/CVF conference on computer vision and pattern recognition*, pages 10684–10695, 2022.
- [49] Duncan A Rowland and David I Perrett. Manipulating facial appearance through shape and color. *IEEE computer graphics and applications*, 15(5):70–76, 1995.
- [50] Nataniel Ruiz, Yuanzhen Li, Varun Jampani, Yael Pritch, Michael Rubinstein, and Kfir Aberman. Dreambooth: Fine tuning text-to-image diffusion models for subject-driven generation. In *Proceedings of the IEEE/CVF Conference on Computer Vision and Pattern Recognition*, pages 22500–22510, 2023.
- [51] Nataniel Ruiz, Yuanzhen Li, Varun Jampani, Wei Wei, Tingbo Hou, Yael Pritch, Neal Wadhwa, Michael Rubinstein, and Kfir Aberman. Hyperdreambooth: Hypernetworks for fast personalization of text-to-image models. *arXiv preprint arXiv:2307.06949*, 2023.
- [52] Simo Ryu. Low-rank adaptation for fast text-to-image diffusion fine-tuning, 2023.
- [53] Florian Schroff, Dmitry Kalenichenko, and James Philbin. Facenet: A unified embedding for face recognition and clustering. In *Proceedings of the IEEE conference on computer vision and pattern recognition*, pages 815–823, 2015.
- [54] Konstantin Schürholt, Dimche Kostadinov, and Damian Borth. Self-supervised representation learning on neural network weights for model characteristic prediction. *Advances in Neural Information Processing Systems*, 34:16481–16493, 2021.
- [55] Viraj Shah, Nataniel Ruiz, Forrester Cole, Erika Lu, Svetlana Lazebnik, Yuanzhen Li, and Varun Jampani. Ziplora: Any subject in any style by effectively merging loras. *arXiv preprint arXiv:2311.13600*, 2023.
- [56] Yujun Shen, Jinjin Gu, Xiaoou Tang, and Bolei Zhou. Interpreting the latent space of gans for semantic face editing. In *Proceedings of the IEEE/CVF conference on computer vision and pattern recognition*, pages 9243–9252, 2020.
- [57] Jascha Sohl-Dickstein, Eric Weiss, Niru Maheswaranathan, and Surya Ganguli. Deep unsupervised learning using nonequilibrium thermodynamics. In *International conference on machine learning*, pages 2256–2265. PMLR, 2015.
- [58] Jiaming Song, Chenlin Meng, and Stefano Ermon. Denoising diffusion implicit models. In *International Conference on Learning Representations*, 2020.
- [59] Omer Tov, Yuval Alaluf, Yotam Nitzan, Or Patashnik, and Daniel Cohen-Or. Designing an encoder for stylegan image manipulation. *ACM Transactions on Graphics (TOG)*, 40(4):1–14, 2021.
- [60] Andrey Voynov and Artem Babenko. Unsupervised discovery of interpretable directions in the gan latent space. In *International conference on machine learning*, pages 9786–9796. PMLR, 2020.

- [61] Kuan-Chieh Wang, Daniil Ostashev, Yuwei Fang, Sergey Tulyakov, and Kfir Aberman. Moa: Mixture-of-attention for subject-context disentanglement in personalized image generation. *arXiv e-prints*, pages arXiv-2404, 2024.
- [62] Kuan-Chieh Wang, Paul Vicol, James Lucas, Li Gu, Roger Grosse, and Richard Zemel. Adversarial distillation of bayesian neural network posteriors. In *International conference on machine learning*, pages 5190–5199. PMLR, 2018.
- [63] Mitchell Wortsman, Gabriel Ilharco, Samir Ya Gadre, Rebecca Roelofs, Raphael Gontijo-Lopes, Ari S Morcos, Hongseok Namkoong, Ali Farhadi, Yair Carmon, Simon Kornblith, et al. Model soups: averaging weights of multiple fine-tuned models improves accuracy without increasing inference time. In *International conference on machine learning*, pages 23965–23998. PMLR, 2022.
- [64] Weihao Xia, Yulun Zhang, Yujiu Yang, Jing-Hao Xue, Bolei Zhou, and Ming-Hsuan Yang. Gan inversion: A survey. *IEEE transactions on pattern analysis and machine intelligence*, 45(3):3121–3138, 2022.
- [65] Guangxuan Xiao, Tianwei Yin, William T Freeman, Frédo Durand, and Song Han. Fastcomposer: Tuning-free multi-subject image generation with localized attention. *arXiv preprint arXiv:2305.10431*, 2023.
- [66] Ge Yuan, Xiaodong Cun, Yong Zhang, Maomao Li, Chenyang Qi, Xintao Wang, Ying Shan, and Huicheng Zheng. Inserting anybody in diffusion models via celeb basis. *Advances in Neural Information Processing Systems*, 36, 2024.
- [67] Kaipeng Zhang, Zhanpeng Zhang, Zhifeng Li, and Yu Qiao. Joint face detection and alignment using multitask cascaded convolutional networks. *IEEE signal processing letters*, 23(10):1499–1503, 2016.
- [68] Richard Zhang, Phillip Isola, Alexei A Efros, Eli Shechtman, and Oliver Wang. The unreasonable effectiveness of deep features as a perceptual metric. In *Proceedings of the IEEE conference on computer vision and pattern recognition*, pages 586–595, 2018.
- [69] Jun-Yan Zhu, Philipp Krähenbühl, Eli Shechtman, and Alexei A Efros. Generative visual manipulation on the natural image manifold. In *Computer Vision—ECCV 2016: 14th European Conference, Amsterdam, The Netherlands, October 11-14, 2016, Proceedings, Part V 14*, pages 597–613. Springer, 2016.

A Sampling

We present additional examples of models sampled from $w2w$ space in Fig. 12. The sampled models encode a diverse array of identities which are not copied from the dataset of model weights, as seen by comparing them to the nearest neighbor models. However, there are attributes borrowed from the nearest neighbors which visually appear in the sampled identity. For instance, the sampled man in the first row shares a similar jawline to the nearest neighbor identity. The sampled identities also demonstrate the same ability as the original training identities to be composed into novel contexts. A variety of prompts are used in Fig. 12, yet the identities are consistent.



Figure 12: **Sampled identity-encoding models from $w2w$ space and their nearest neighbor models.** The sampled identities share some characteristics with the nearest neighbors, but are still distinct. These identities can also be composed into novel contexts like a standard customized diffusion model.

B Composing Edits

We display additional examples of applying edits in $w2w$ space based on the directions discovered using linear classifiers and CelebA labels. In Fig. 13, we demonstrate how the strength of these edits can be modulated and combined with minimal interference. These edits are apparent even in more complex scenes beyond face images. Also, the edits do not degrade other present concepts, such as the dog near the man (top left example).

In Figs. 14 and 15, we demonstrate how multiple edits can be progressively added in a disentangled fashion with minimal degradation to the identity. Additionally, since we operate in a subspace of weight space, these edits persist with a consistent appearance across different generations. For instance, even the man exhibits the edits as a painting in Fig. 14.

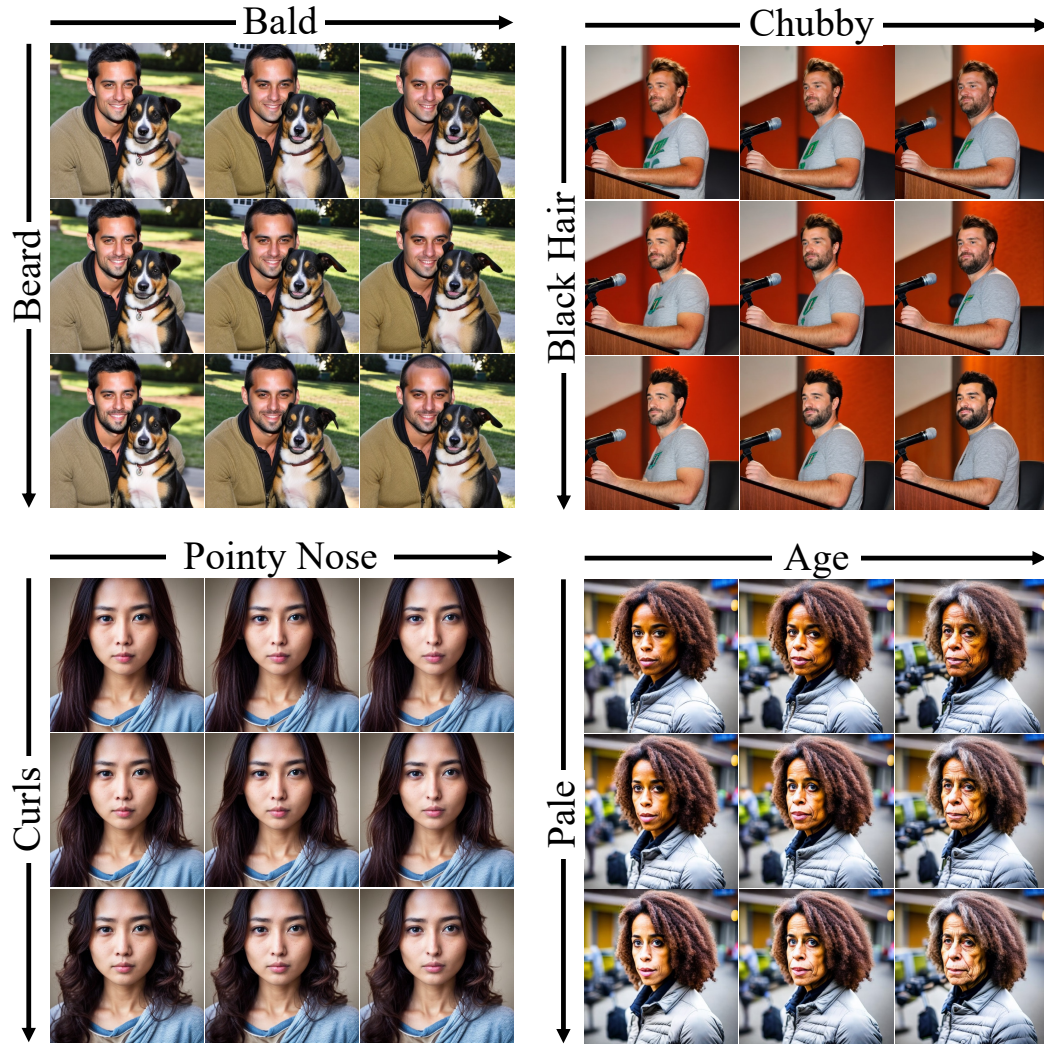


Figure 13: Multiple edits can be controlled in a continuous manner.



Figure 14: **Composing four different edits with minimal identity degradation.** These edits bind to the identity and persist in appearance across multiple generation seeds and prompts.



Figure 15: **Additional examples of composing multiple edits.** We provide more examples of semantic edits based on labels available from CelebA.

C Inversion

We present additional details on $w2w$ inversion and comparisons against training Dreambooth LoRA on a single image vs. multiple images.

Implementation Details: To conduct $w2w$ inversion, we train on a single image following the objective from eq. 3. We qualitatively find that optimizing 10,000 principal component coefficients balances identity preservation with editability. This is discussed in Appendix F. We optimize for 400 epochs, using Adam [28] with learning rate 0.1, $\beta_1 = 0.9$, $\beta_2 = 0.999$ and with weight decay factor $1e-10$. For conducting Dreambooth fine-tuning, we follow the implementation from Hugging Face³ using LoRA with rank 1. To create a dataset of multiple images for an identity, we follow the procedure from Sec. 4.4.

$w2w$ inversion is more efficient than previous methods. Inversion into $w2w$ space results in a significant speedup in optimization as seen in Tab. 3, where we measure the training time on a single NVIDIA A100 GPU. Standard Dreambooth fine-tuning operates on the full weight space and incorporates an additional prior preservation loss which typically requires hundreds of prior images. In contrast, we only optimize a standard denoising objective on a single image within a low-dimensional weight subspace. Despite operating with lower dimensionality, $w2w$ inversion performs closely to standard Dreambooth fine-tuning on multiple images with LoRA.

Table 3: **Inversion into $w2w$ space balances identity preservation and efficiency.**

Method	Single-Image	# Param	Opt. Time (s)	Identity Fidelity \uparrow
DB-LoRA	×	99,648	220	0.69 ± 0.01
DB-LoRA	✓	99,648	200	0.43 ± 0.03
$w2w$ Inversion	✓	10,000	55	0.64 ± 0.01

Qualitative Inversion Comparison. In Figs. 16 and 17, we present qualitative comparisons of $w2w$ inversion against Dreambooth trained with multiple images and a single image. Although *multi-image* Dreambooth slightly outperforms $w2w$ inversion in identity preservations, its samples tend to lack realism compared to $w2w$ inversion. We hypothesize that this may be due to using generated images for prior preservation and training on synthetic identity images. Dreambooth trained on a single image either generates an artifacted version of the original image or random identities. Notice how inversion into $w2w$ space is even able to capture key characteristics of the child although babies are nearly to completely absent in the identities based on CelebA used to fine-tune our dataset of models.

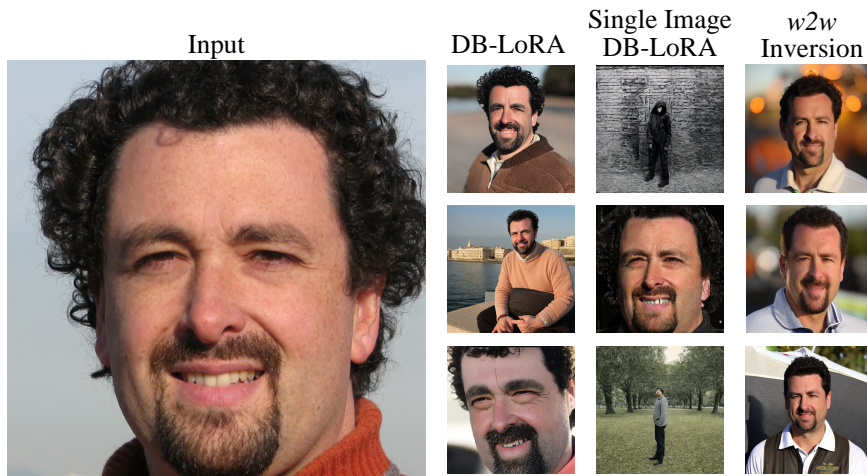


Figure 16: **Inversion into $w2w$ space preserves identity and realism.** We compare against Dreambooth fine-tuning with LoRA on multiple images and a single image.

³<https://github.com/huggingface/peft>

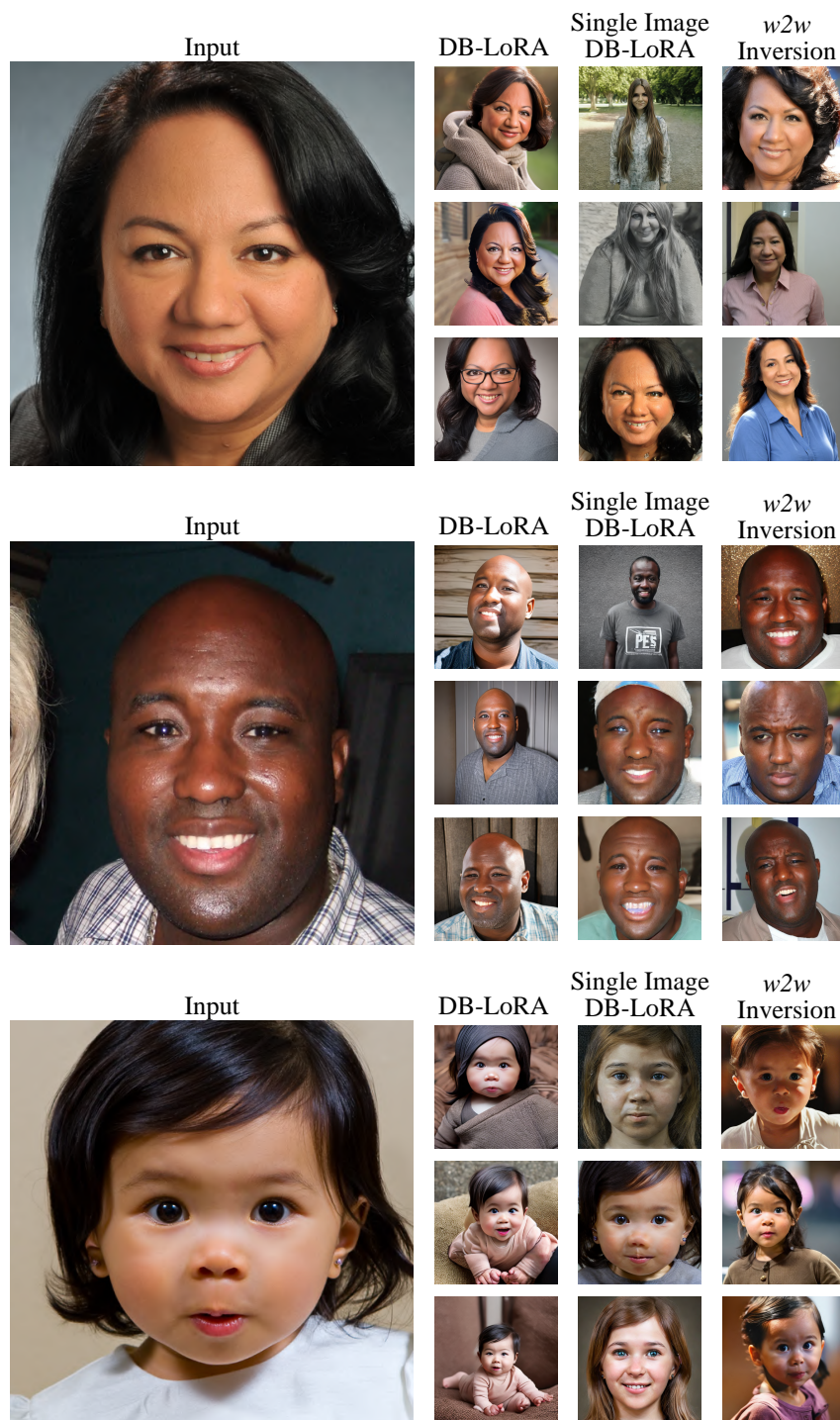


Figure 17: Inversion into $w2w$ space preserves identity and realism (cont.).

D Out of Distribution Projection

Additional examples of out-of-distribution projections are displayed in Fig. 18. A diverse array of styles and subjects (e.g. paintings, sketches, non-humans) can be distilled into a model in $w2w$ space. After embedding an identity into this space, the model still retains the compositionality and rich priors of a standard personalized model. For instance, we can generate images using prompts such as “[v] person writing at a desk” (top example), “[v] person with a dog” (middle example), or “a painting of [v] person painting on a canvas” (bottom example).

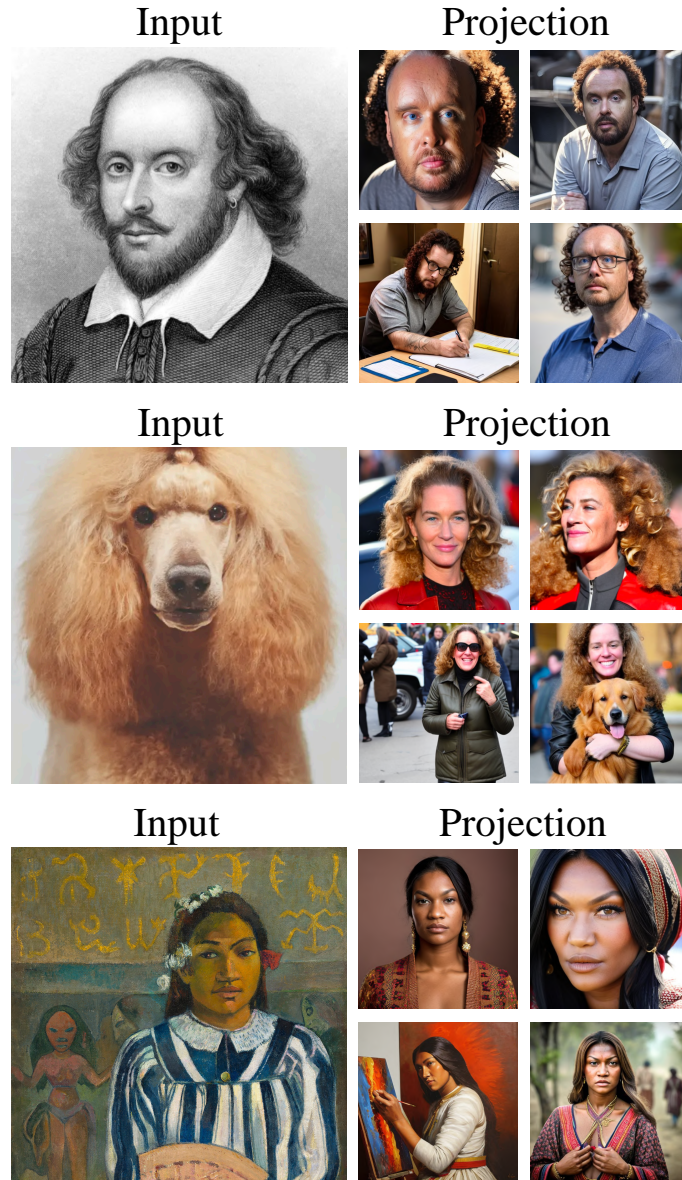


Figure 18: **Projection into $w2w$ space generalizes to a variety of inputs.** A range of styles and entities can be inverted into a realistic identity in this space. Once a model is obtained, it can be prompted to generate the identity in a variety of contexts.

E Identity Datasets

In Fig. 19, we present examples of synthetic identity datasets used to conduct our Dreambooth fine-tuning as discussed in Sec 4. Each dataset is a set of ten images generated with [61] conditioned on a single CelebA [33] images associated with binary attribute labels. Note that we only display a subset of images per identity in the figure. Creating these synthetic datasets reduces intra-dataset diversity and creates a more consistent appearance for each subject. For instance, the first two rows in the figure are the same identity, but look drastically different. So we instead treat them as different identities associated with a different set of images.

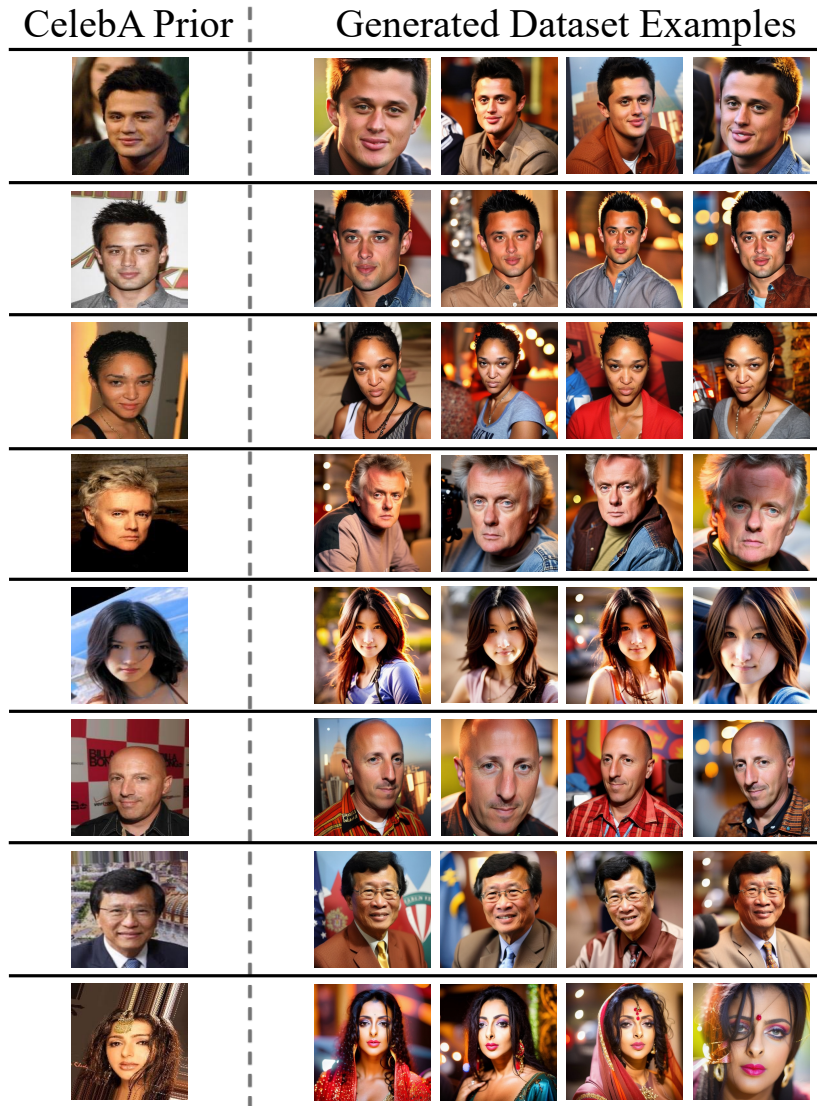


Figure 19: **Fine-tuning on synthetic examples allows Dreambooth fine-tuning to distill a consistent identity.** The left column shows a CelebA image used to condition generation of a set of identity-consistent images in the right column associated with that identity. The consistent appearance of the identity enables a more consistent identity encoding.

F Principal Component Basis

In this section, we analyze various properties of the Principal Component (PC) basis used to define w_{2w} Space. We investigate the distribution of PC coefficients and the effect of the number of PCs on identity editing and inversion.

Distribution of PC Coefficients. We plot the histogram of the coefficient values for the first three Principal Components in Fig. 20. They appear roughly Gaussian. Next, we rescale the coefficients for these three components to unit variance for visualization purposes. We then plot the pairwise joint distributions for them in Fig. 21. The circular shapes indicates roughly diagonal covariances. Although the joint over other combinations of Principal Components may exhibit different properties, these results motivate us to model the PCs as independent Gaussians, leading to the w_{2w} sampling strategy from Sec. 3.2.

Number of Principal Components for Identity Editing We empirically observe that training classifiers based on the 1000 dimensional PC representations (first 1000 PCs) of the model weights results in the most semantically aligned and disentangled edits directions. We visualize a comparison for the “goatee” direction in Fig. 22. After finding the direction, we calculate the maximum projection component onto the edit direction among the training set of model weights. This determines the edit strength. As seen in the figure, restricting to the first 100 Principal Components may be too coarse to achieve the fine-grained edit, instead relying on spurious cues such as skin color. Training with the first 10,000 Principal Components suffers from the curse of dimensionality and the discovered direction may edit other concepts such as eye color or clothes. Finding the direction using the first 1000 Principal Components achieves the desired edit with minimal entanglement with other concepts.

Number of Principal Components for Identity Inversion We qualitatively observe that inverting into w_{2w} Space using the first 10,000 Principal Components balances identity preservation while not overfitting to the source image. We visualize a comparison in Fig. 23, where each column has a fixed seed and prompt. Optimizing with the first 1000 PCs underfits the identity and does not generate a consistent identity. Inversion with the first 20,000 Principal Components overfits to the source image of a face shot, which results in artifacted face images despite different generation seeds and prompts. Optimizing with the first 10,000 Principal Components enjoys the benefits of a lower dimensional representation than the original LoRA parameter space ($\sim 100,000$ trainable parameters), while still preserving identity and compositionality.

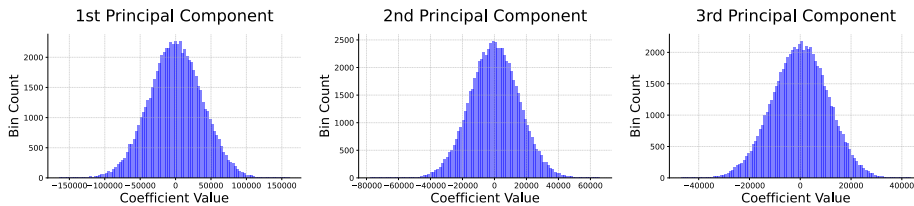


Figure 20: **Histogram of Principal Component Coefficients.** The first three Principal Component coefficients appear approximately Gaussian.

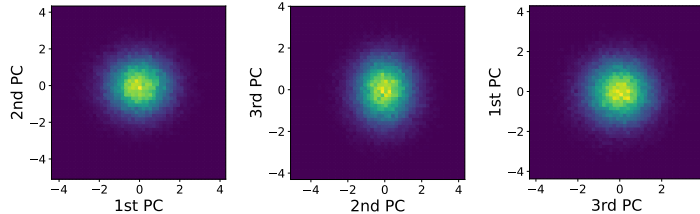


Figure 21: **Pairwise Joint Histogram of Principal Component Coefficients.** We rescale the first three principal component coefficients and plot the pairwise joint distributions for visualization purposes. Given that the marginals are roughly Gaussian, the circular appearance of the joint suggests pairwise independence for the first three components.

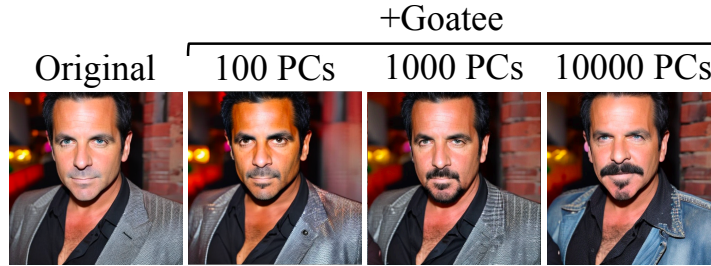


Figure 22: **Edit results with varying number of Principal Components.** Training classifiers to find semantic weight space directions with the first 1000 Principal Components achieves the most semantically aligned and disentangled results.

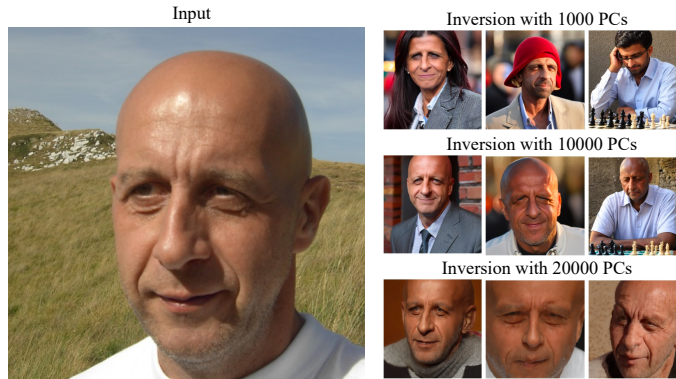


Figure 23: **Identity inversion results with varying number of Principal Components.** We optimize the coefficients for the first 1000, 10000, and 20000 Principal Component coefficients. Each column indicates a fixed generation seed and prompt. Inversion with the first 10,000 components balances parameter efficiency, realism, and identity preservation, and without overfitting to the single image.

G Timestep Analysis

Edits in $w2w$ Space correspond to identity edits with minimal interference with other visual concepts. Although not a focus, image editing is achieved as a byproduct. For further context preservation, edits in $w2w$ Space can be integrated with delayed injection [5, 14, 32, 65], where after T timesteps, the edited weights are used instead of the original ones. We visualize this in Fig. 24. Larger T in the range [700, 1000] are helpful for more global attribute changes, while smaller [400, 700] can be used for more fine-grained edits. However, by decreasing the timestep T , the strength of the edit is lost in favor of better context preservation. For instance, the dog’s face is better preserved in the second row at $T = 600$, although the man is not as chubby compared to other T .

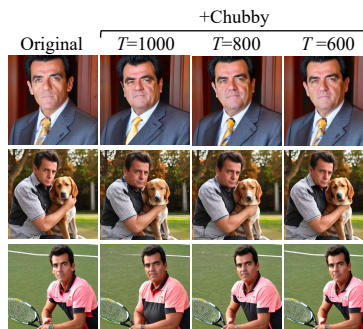


Figure 24: **Injecting the edited weights at a lower timestep T better preserves context at the expense of edit strength and fidelity.**

H Extending to Other Domains

We find that similar subspaces can be created for other visual concepts beyond human identities. For instance, we apply the *weights2weights* framework to models encoding different dog breeds. We generate images with Stable Diffusion based on each of the 120 dog classes from ImageNet [9]. We then conduct Dreambooth finetuning on each set of images to create a dataset of 120 dog-encoding models. To find edit directions, we use GPT-4 [2] to create labels for each dog breed (e.g., wavy hair or not) and then train linear classifiers on the model weights like Sec. 3.3. We present examples of editing the dog-encoding models in Fig. 25. These hint at the generality of *weights2weights*, although more visual concepts should be explored to make a concrete conclusion.

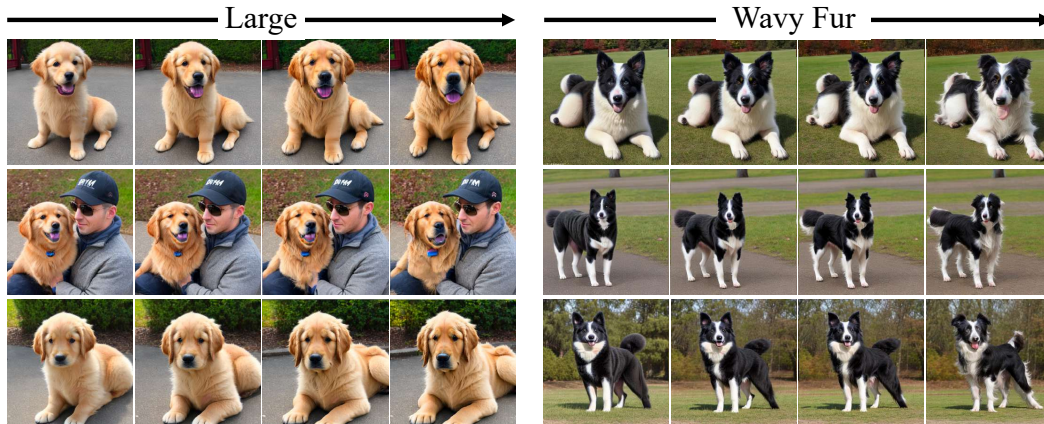


Figure 25: **Applying *weights2weights* edits on dog-encoding models.** This suggests that *weights2weights* space can be constructed on domains beyond human identities.